Thermal Degradation Kinetics of Poly(propylene carbonate) Obtained from the Copolymerization of Carbon Dioxide and Propylene Oxide

Binyuan Liu, Xiaojiang Zhao, Xianhong Wang, Fosong Wang

State Key Laboratory of Polymer Physics and Chemistry and Open Laboratory of Polymer Chemistry, Changchun Institute of Applied Chemistry, Chinese Academy of Sciences, Changchun, 130022, People's Republic of China

Received 4 September 2002; accepted 17 December 2002

ABSTRACT: The kinetics of the thermal degradation of poly(propylene carbonate) (PPC) were investigated with different kinetic methods with data from thermogravimetric analysis under dynamic conditions. The apparent activation energies obtained with different integral methods (Ozawa–Flynn–Wall and Coats–Redfern) were consistent with the values obtained with the Kinssinger method (99.93 kJ/mol). The solid-state decomposition process was a sigmoidal A_3 type in terms of the Coats–Redfern and Phadnis–Deshpande results. The influence of the heating rate on the thermal decomposition temperature was also studied. The derivative thermogravimetry curves of PPC confirmed only one weight-loss step. © 2003 Wiley Periodicals, Inc. J Appl Polym Sci 90: 947–953, 2003

Key words: copolymerization; thermogravimetric analysis (TGA); activation energy; thermodynamics

INTRODUCTION

Poly(propylene carbonate) (PPC), which can be synthesized by the copolymerization of carbon dioxide and propylene epoxide, as reported in many publications,[1–3] is an aliphatic polycarbonate with reasonably good mechanical and biodegradable properties and a potentially wide range of applications,[4–6] such as binder resins, packing materials, adhesives, biodegradable materials, and ceramic processing. Therefore, it is important to investigate the thermal stability of this type of carbon dioxide-based resin because it can determine the final properties of the material, such as the upper temperature limit, the machining process, the mechanism of the solid-state process, and the lifetime.

Thermogravimetric analysis (TGA) records the mass change of a sample as a function of temperature or as a function of time at a given heating rate (Φ).[7] With thermogravimetric curves, many studies of thermogravimetric data have been used for the estimation of the kinetic parameters of degradation processes, such as rate constants, activation energies, reaction orders, and the Arrhenius pre-exponential factor (A). Although these kinetic parameters depend on factors such as the nitrogen atmosphere, sample mass, sample shape, flow rate, Φ, and particle of the sample (especially Φ),[8–10] TGA has widely been used because of its simplicity and the information obtained from a simple thermogram. In fact, many kinetic analytical methods have been based on the scanning rate dependence of TGA data.[11–13]

In this article, the thermal degradation of PPC was investigated with dynamic thermogravimetry (TG). One objective was to study the effect of Φ on the thermal decomposition temperature (T) and weight-loss percentage (a). The other objective was to investigate the kinetics of the thermal degradation of PPC with different kinetic methods (differential and integral) under nonisothermal conditions, including the mechanism and apparent activation energy of thermal degradation.

THEORETICAL BACKGROUND[12,14,15]

In the reaction $B(s) \rightarrow D(s) + C(g)$, where $B(s)$ is the starting material, $D(s)$ and $C(g)$ are the different products during the disappearance of $B(s)$, the disappearance rate ($d\alpha/dt$) can be defined as follows:

$$\frac{da}{dt} = kf(a) \tag{1}$$

where α is a fraction of B decomposed at time t and $f(\alpha)$ is a temperature-independent function of conversion α. k is the rate constant given by the Arrhenius equation:

$$k = A \exp(-E/RT) \tag{2}$$

Correspondence to: X. Wang (xhwang@ns.ciac.jl.cn).

Contract grant sponsor: Chinese Academy of Sciences.
Contract grant sponsor: National Natural Science Foundation of China; contract grant number: 50003009.

TABLE I
Algebraic Expressions for *g(a)* for the Most Frequently Used Mechanisms of Solid-State Processes[14,22]

Symbol	*g(a)*	Solid-state processes
Sigmoidal Curves		
A_2	$[-\ln(1 - a)]^{1/2}$	Nucleation and growth [Avrami–Erofeev, eq. (1)]
A_3	$[-\ln(1-a)]^{1/3}$	Nucleation and growth [Avrami–Erofeev, eq. (2)]
A_4	$[-\ln(1 - a)]^{1/4}$	Nucleation and growth [Avrami–Erofeev, eq. (3)]
Decleration Curves		
R_1	a	Phase-boundary-controlled reaction (one-dimensional movement)
R_2	$2[1 - \ln(1 - a)^{1/2}]$	Phase-boundary-controlled reaction (contracting area)
R_3	$3[1 - \ln(1 - a)^{1/3}]$	Phase-boundary-controlled reaction (contracting volume)
D_1	a^2	One-dimensional diffusion
D_2	$(1 - a)\ln(1 - a) + a$	Two-dimensional diffusion (Valensi equation)
D_3	[1−(1−a)1/3]2	Three-dimensional diffusion (Jander equation)
$D4$	$\left(1 - \frac{2}{3}a\right) - (1 - a)^{2/3}$	Three-dimensional diffusion (Ginstling–Brounshtein equation)
F_1	$-\ln(1 - a)$	Random nucleation with one nucleus on the individual particle
F_2	$\frac{1}{1-a}$	Random nucleation with two nuclei on the individual particle
F_3	$\frac{1}{(1-a)^2}$	Random nucleation with two nuclei on the individual particle

where A is the frequency factor or pre-exponential factor and E is the activation energy of the reaction. Substituting the Arrhenius equation into eq. (1), we obtain

$$\frac{da}{dt} = A \exp(-E/RT)f(a) \tag{3}$$

If the temperature of a sample is changed by a controlled and constant value of Φ ($\Phi = dT/dt$), the variation of the degree of conversion can be analyzed as a function of temperature, which depends on the time of heating.

Therefore, the reaction rate gives

$$\frac{da}{dT} = \frac{A}{\phi} \exp(-E/RT)f(a) \tag{4}$$

Separating the variable and rearranging and integrating eq. (4), we obtain

$$g(a) = \int_{a_o}^{a_p} \frac{da}{f(a)} = \frac{A}{\phi} \int_{T_o}^{T_p} \exp(-E/RT)\, dT \tag{5}$$

If we define $x = E/RT$ and integrate the right-hand side of eq. (5), we obtain

$$\frac{A}{\Phi} \int_{T_o}^{T_p} \exp(-E/RT)\, dT = \frac{AE}{\phi T}\, p(x) \tag{6}$$

After taking logarithms, we obtain

$$\log \Phi = \log \frac{AE}{g(a)R} + \log p(x) \tag{7}$$

where $p(x) = (e^{-x}/x^2)\ \Sigma_{n=1}\ (-1)^{n-1}\ (n!/x^{n-1})$ and $g(a)$ is the function of conversion. The function $p(x)$ can be expressed by some approximate equation when x meets certain conditions.

For polymers, the integral function $g(a)$ is either a sigmoidal function or a deceleration function. Table I presents different expressions of $g(a)$ for the different solid-state mechanisms.[10] These functions adequately estimated the reaction solid-state mechanism for nonisothermal TG experiments.

In this article, we use different mathematical treatments to explain the previous equation. For the integral methods, we use an approximate integration of eq. (6) with different mathematics. These methods are now described.

Kinssinger method[13]

This method derives from the correlation between the peak temperature (T_p) and Φ. Suited for more than four thermal analytical curves of the derivation type, it is an efficient differential method. With this method, the apparent activity energy can be estimated without a precise knowledge of the reaction mechanism:

$$\ln \frac{\Phi}{T_p^2} = \left\{\ln \frac{AR}{E} + \ln[n(1 - a_p)^{n-1}]\right\} - \frac{E}{RT_p} \tag{8}$$

where T_p is the temperature corresponding to the maximum weight-loss rate, a_p is the maximum con-

version, and n is the reaction order. Φ, A, and E have already been defined.

The following three kinds of methods are integral methods.

Ozawa–Flynn–Wall method[11]

This method uses the Doyle approximation,[15] that is, when $20 \leq x \leq 60$ is true, the function $p(x)$ can be adopted into the following approximation:

$$\log p(x) \approx -2.315 - 0.4567x \tag{9}$$

Substituting eq. (9) to eq. (7), we obtain

$$\log \Phi = \log \frac{AE}{g(a)R} - 2.315 - \frac{0.4567E}{RT} \tag{10}$$

Therefore, if a series of experiments are run at different values of Φ, the apparent activation energy (E) can be obtained from a plot of $\log \Phi$ against $1/T$ for a fixed degree of conversion. The slope of such a line is given by $-0.4567E/R$ (where R is a correlation coefficient) without knowledge of the reaction order.

Coats–Redfern method[12]

The Coats–Redfern method uses an asymptotic approximation for the resolution of eq. (5) at different conversion values. If $(2RT)/E \rightarrow 0$ is true for the Doyle approximation,[15] we obtain in a natural logarithmic form

$$\ln \frac{g(a)}{T^2} = \ln \frac{AR}{\Phi E} - \frac{E}{RT} \tag{11}$$

According to the different degradation processes, with the theoretical function $g(a)$, which is listed in Table I,[10] we can obtain the apparent activity energy and frequency factor from the slope of the plot, $\ln[g(a)/R^2]$ versus $1/T$, as well as the valid reaction mechanism.

Phadnis–Deshpande method[16]

When taking function $p(x)$ as two former terms, we obtain:

$$g(a) = \frac{ART^2}{\Phi E}\left[1 - \frac{2RT}{E}\right]\exp(-E/RT) \tag{12}$$

Rewriting eq. (12) by substituting eq. (4) and rearranging it, we obtain

$$f(a)g(a) = \frac{RT^2}{E}\left(1 - \frac{2RT}{E}\right)\frac{da}{dT} \tag{13}$$

Passing over the comparatively small term $2R^2T^3/E^2$, we can shorten eq. (13):

TABLE II
$g'(a)$ for Frequently Used Solid-State Reaction Mechanisms in the Phadnis–Deshpande Method[16]

$g'(a)$	Reaction mechanism
$\ln a$	Power law (1)
$2 \ln a$	Power law (2)
$\ln[1 - (1 - a)^{1/3}]$	Phase boundary (contracting sphere; 3)
$\ln[1 - (1 - a)^{1/2}]$	Phase boundary (contracting cylinder; 4)
$\frac{1}{2}\ln[-\ln(1 - a)]$	Nucleation and nuclei growth (5; Avrami–Erofeev nuclei growth)
$\frac{1}{3}\ln[-\ln(1 - a)]$	Nucleation and nuclei growth (6; Avrami–Erofeev nuclei growth)
$\frac{1}{4}\ln[-\ln(1 - a)]$	Nucleation and nuclei growth (7; Avrami–Erofeev nuclei growth)
$\ln[(1 - a)\ln(1 - a) + a]$	Valensi two-dimensional diffusion (8)
$2 \ln[1 - (1 - a)^{1/3}]$	Jander, three-dimensional diffusion (9)
$\ln[1-\frac{2}{3}a-(1-a)^{2/3}]$	Brounshtein–Ginstling, three-dimensional diffusion (10)

$$f(a)g(a) = \frac{RT^2}{E}\frac{da}{dT} \tag{14}$$

Alternatively, with the integration of eq. (14), we obtain

$$g'(a) = -\frac{E}{RT} \tag{15}$$

where $g'(a)$ is equal to $\int f(a)g(a)da$. The integral function $g'(a)$ is listed in Table II.

This method can determine the dependence of reaction mechanism on the functional form of a based on the linearity of the plot of $f(a)$ and $g(a)$ versus T^2da/dT, or $g'(a)$ against $1/T$ and the apparent activity energy, which can be obtained by other methods (in this study, with the Kinssinger and Ozawa–Flynn–Wall methods). The plot of $g'(a)$ versus $1/T$ is linear with the proper functional form of a. The slope of this plot, if multiplied by R, gives the value of E. The application of a method such as the Coats–Redfern method gives a means of acquiring the valid reaction mechanism.

EXPERIMENTAL

Materials

The PPC resin was synthesized from the copolymerization of carbon dioxide and propylene oxide according to the literature.[17,18] The number-average molecular weight and polydispersity of PPC were 1.3×10^4 and 3.4, re-

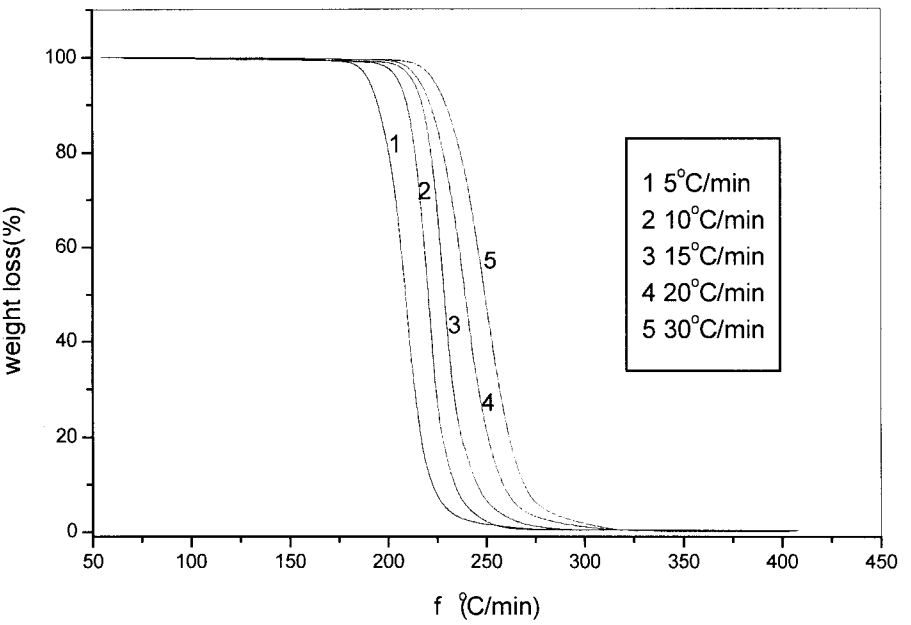

(a)

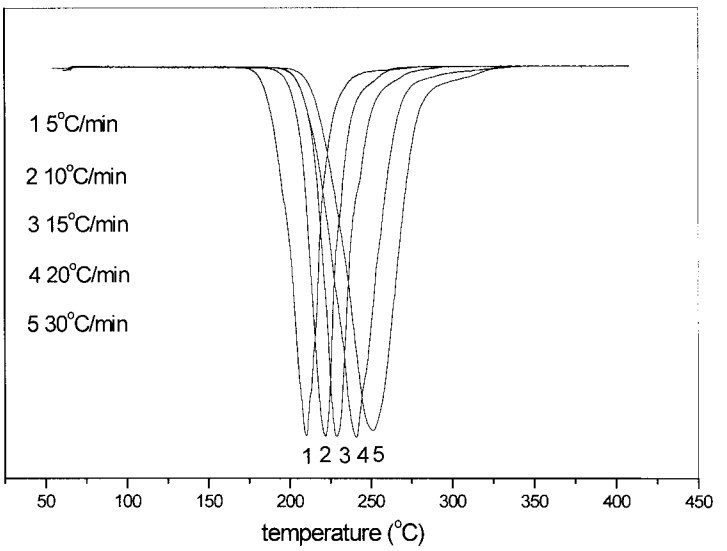

(b)

Figure 1 (a) TG and (b) DTG curves of PPC thermal degradation at different values of Φ.

spectively, as measured with a gel permeation chromatography system on a Waters 400 spectrometer (Milford, USA), with tetrahydrofuran as an eluent.

TGA

TGA was performed with a PerkinElmer TGA7 (New York) instrument. The polymer sample (9.5 ± 0.5 mg) was stacked in an open platinum sample pan, and the experiment was conducted under a nitrogen gas atmosphere with various values of Φ (5, 10, 15, 20, and 30°C/min) from 60–400°C to obtain the residual weight curves of the PPC resin. The nitrogen gas rate was 20 mL/min.

RESULTS AND DISCUSSION

Figure 1(a,b) illustrates the TG and derivative thermogravimetry (DTG) curves, respectively, from the thermal decomposition of PPC at different Φ values. The TG curves were smooth weight-loss curves. The DTG curves showed only a maximum-weight-loss-rate (da/dt) peak. This indicated that the decomposition corresponded to a single-stage decomposition reaction in which the values of decomposition temperature (T) were well defined. With increases in Φ, the TG and DTG curves shifted toward the high-temperature zone. The decomposition behaviors at all Φ values were similar.

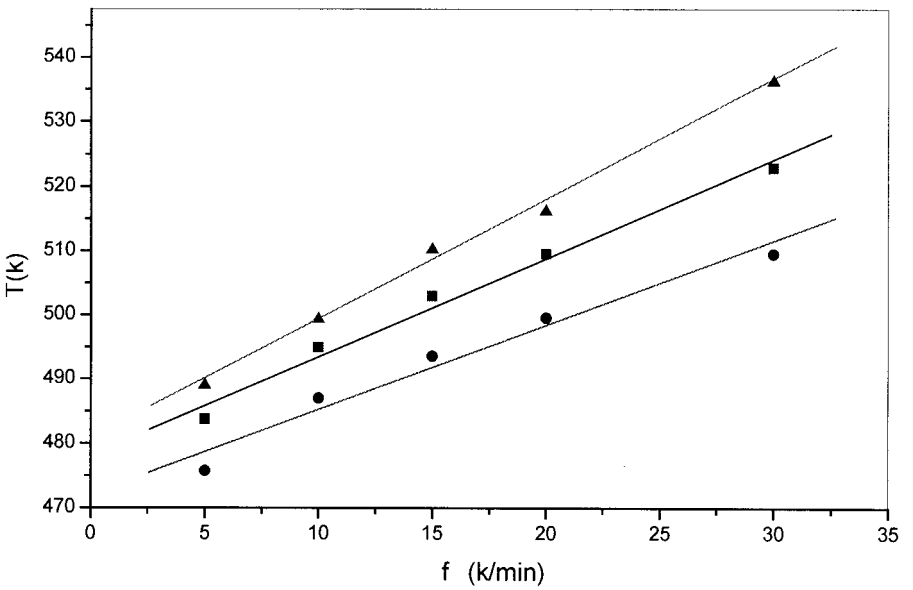

Figure 2 Relationship of T and Φ for PPC: (▲) T_f, (■) T_p, and (●) T_0.

Figure 2 presents the influence of Φ on T. The temperature at the onset of weight loss (T_i) and the temperature of the final decomposition (T_f) were obtained from the TG curve with the tangent method. T_p, the minimum of the DTG curve peak, is shown. Figure 2 shows that T increased with Φ, indicating that Φ was the important factor affecting T. These factors were related as follows:

$$T_i = 472.8 + 1.23\Phi$$
$$T_p = 478.4 + 1.53\Phi$$
$$T_f = 480.5 + 1.85\Phi$$

The increase in T with increasing Φ was the result of the heat lag of the process.[19] T can be expressed more exactly as $[T(0)]$ when Φ is approximately zero: $T_i(0) = 472.8$ K, $T_p(0) = 478.4$ K, and $T_f(0) = 480.5$ K.

EVALUATION OF THE ACTIVATION ENERGY

With the Kinssinger method[13] and the experimental data measured in the TG curves (Fig. 1), the activation energy for the decomposition of the PPC system was estimated from the slope of a straight line of $\ln(\Phi/T_p^2)$ versus $1000/T_p$, as shown in Figure 3. From the slope

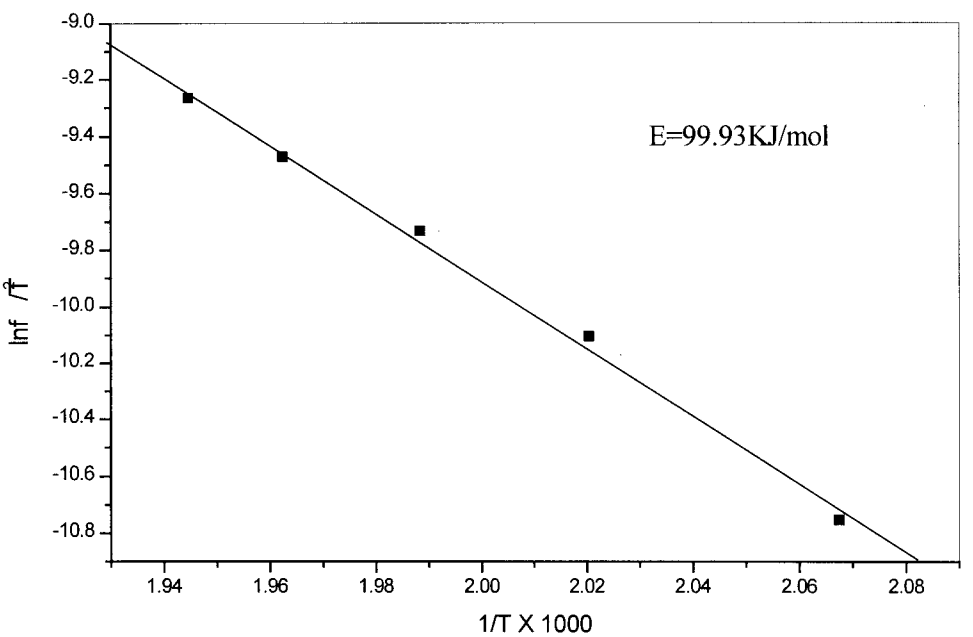

Figure 3 Kinssinger method applied to experimental data at different values of Φ.

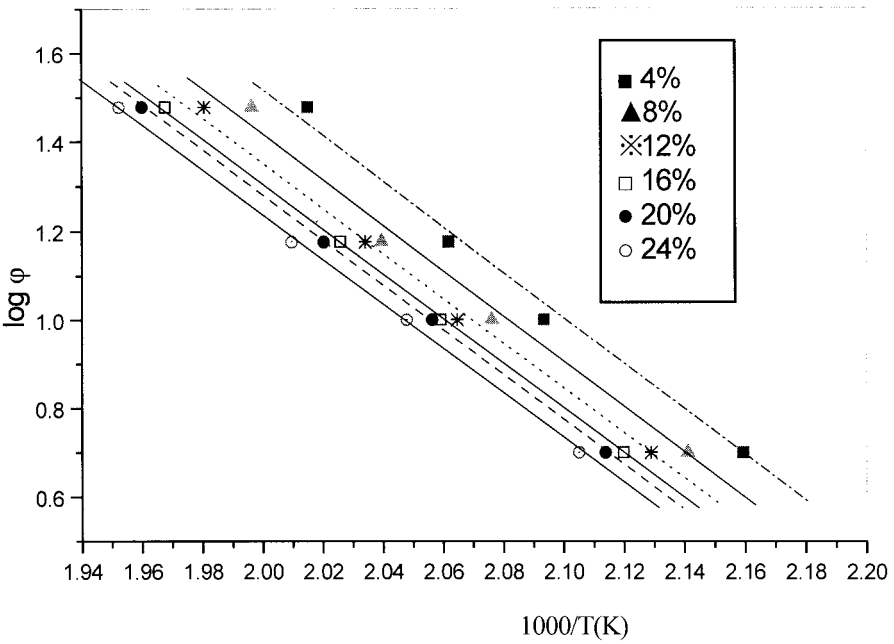

Figure 4 Typical plots of log Φ versus $1000/T$ at several conversions in the range of 4–24% in steps of 4% (Ozawa–Flynn–Wall method).

of the plot, the apparent activation energy could be calculated as E = Slope × R = 99.93 kJ/mol. The apparent activation energies were also evaluated with the Ozawa–Flynn–Wall method. It was applicable to integral-type DTG curves. According to eq. (9), the plot of log Φ versus $1000/T$ at a given conversion gave a straight line. In this case, we used Φ values of 5, 10, 15, and 30°C/min. Figure 4 shows nearly parallel fitted straight lines, indicating the applicability of this method to our system in the conversion range studied. Table III shows the activation energies corresponding to different conversions. From these values, a mean value of 94.42 kJ/mol was obtained. By the comparison of this last value with the activation energy calculated with the Kinssinger method, a difference of 5.51 kJ/mol was found.

These two methods have the advantage of not requiring previous knowledge of the reaction mechanism for solving the activation energy. Therefore, some authors[20,21] have used the activation energies obtained with these methods to validate their thermal degradation mechanism models.

TABLE III
Activation Energies (E_s) Obtained with the Ozawa–Flynn–Wall Method

a (%)	E (kJ/mol)	R
4	97.43	0.99584
8	96.30	0.99442
12	95.61	0.99854
16	93.21	0.9999
20	91.93	0.99989
24	92.17	0.99973

Many mathematical methods have been postulated in the literature[14,22] for the affirmation of the mechanism of a solid-state reaction from thermoanalytical curves obtained isothermally or nonisothermally. In general, the correlation coefficient of a plot for different mechanism functions has been regarded as standard for the determination of the reaction mechanism, but sometimes the correlation coefficients of the lines have slight differences; in this case, it is necessary to determine the mechanism in terms of other supplementary methods.[23] We used the Coats–Redfern method and Phadnis–Deshpande method to investigate the model of the PPC decomposition by comparing the activation energy values with the Kinssinger method or Ozawa–Flynn–Wall method calculations by way of the relative linearity of the plot.

TABLE IV
Activation Energies (E_s) Obtained with the Coats–Redfern Method for Several Solid-State Processes at 5°C/min

Mechanism	E (kJ/mol)	R
A_2	153.14	0.9966
A_3	99.52	0.9964
A_4	72.66	0.9962
R_1	295.06	0.9957
R_2	10.56	0.9857
R_3	4.66	0.9657
D_1	598.03	0.9958
D_2	610.49	0.9962
D_3	623.38	0.9965
D_4	614.90	0.9963
F_1	314.27	0.9967
F_2	31.34	0.9910
F_3	70.50	0.9928

TABLE V
Activation Energies (E_s) of PPC Thermal Degradation Obtained with the Phadnis–Deshpande Method at 5°C/min

Reaction mechanism	E (kJ/mol)	R
Power law (1)	302.88	0.9959
Power law (2)	605.84	0.9959
Phase boundary (3)	315.60	0.9966
Phase boundary (4)	312.36	0.9964
Nucleation and growth [5; Avrami, eq. (1)]	161.04	0.9969
Nucleation and growth [6; Avrami, eq. (2)]	107.33	0.9969
Nucleation and growth [7; Avrami, eq. (3)]	80.48	0.9969
Valensi, two-dimensional diffusion (8)	618.31	0.9963
Jander, three-dimensional diffusion (9)	631.20	0.9966
Brounshtein–Ginstling, three-dimensional diffusion (10)	622.64	0.9964

The apparent activation energy corresponding to different $g(a)$ values for sigmoidal and decelerated mechanisms (Table I) could be obtained at constant values of Φ with the Coats–Redfern equation from a fitting of $\ln[g(a)/T^2]$–$1000/T$ plots. Table IV shows the activity energies and correlation at Φ = 5°C/min. The linearity of the plot of $\ln[g(a)/T^2]$ versus $1000/T$ for R_2, R_3, F_2, and F_3 was bad. Therefore, when we examined the correlation coefficient (good plot linearity) as the standard, R_2, R_3, F_2, and F_3 degradation processes were excluded first. In addition, when we compared the activation energies in Table IV, at Φ = 5°C/min, we found that the apparent activation energies were in good agreement with those obtained from the Kinssinger method and Ozawa–Flynn–Wall method (A_n-type mechanism). Table IV shows that the best agreement occurred when the activation energy corresponding to A_3 was 99.52 kJ/mol, very close to the value of 99.93 kJ/mol obtained from the Kinssinger method, indicating that the pyrolysis of PPC probably followed a sigmoidal (A_n) type; that is, the rate-controlling process obeyed the random nucleation Avrami–Erofeev equation .

To further confirm the thermal degradation behavior, we also calculated the apparent activation energies via the Phadnis–Deshpande method in its integral form at Φ = 5°C/min. The values of the activation energies according to this method are listed Table V. From Table V, it can be seen that the correlations of all the plots were good, but only when the thermal process obeyed the Avrami–Erofeev equation [eq. (2); Table II]; the value of the apparent activation energy of PPC degradation was calculated to be 107.33 kJ/mol, close to the values from the Kinssinger and Ozawa–Flynn–Wall methods. This result further supported the A_n-type mechanism.

Finally, both the Coats–Redfern method and Phadnis–Deshpande method led to plots with good linearity with all functional forms of a, except for R_2, R_3, F_2, and F_3 with the Coats–Redfern method. In other words, it was difficult to obtain the exact reaction mechanism for the thermal degradation of PPC with only the correlation coefficient of a plot based on either eq. (11) or eq. (15).

CONCLUSIONS

The effects of Φ on T were studied, and we found that the degradation temperature increased with an increase in Φ and that the PPC thermal degradation proceeded via a one-step process. The apparent activation energies of the PPC thermal degradation calculated with the Kinssinger method and Ozawa–Flynn–Wall method were in good agreement with each other. A sigmoidal A_n-type thermal degradation mechanism for PPC was followed according to the Coats–Redfern and Phadnis–Deshpande methods.

References

1. (a) Inoue, S.; Koinuma, H.; Tsuruta, T. J Polym Sci Part B: Polym Lett 1969, 7, 287; (b) Inoue, S.; Koinuma, H.; Tsuruta, T. Makromol Chem 1969, 130, 210.
2. Rokicki, A.; Kuran, W. J Macromol Sci Rev Macromol Chem 1981, 21, 135.
3. Super, M. S.; Beckman, E. J. Trends Polym Sci 1997, 5, 236.
4. Ree, M.; Bae, J. Y.; Shin, T. J. J Polym Sci Part A: Polym Chem 1999, 37, 1863.
5. Beckman, E. J. Science 1999, 283, 946.
6. Bronk, J. M.; Riffle, J. S. Polym Prepr 1994, 35(1), 815.
7. Hatakeyama, T.; Liu, Z. H. Handbook of Thermal Analysis; Wiley: Chichester, England, 1998; p 17.
8. Hatakeyama, T.; Liu, Z. H. Handbook of Thermal Analysis; Wiley: Chichester, England, 1998; pp 42–46.
9. Cameron, G. G.; Rudin, A. J Polym Sci Polym Phys Ed 1981, 19, 1799.
10. MacCallum, J. R. Br Polym J 1979, 11, 12.
11. Ozawa, T. Bull Chem Soc Jpn 1965, 38, 1881.
12. Coats, A. W.; Redfern, J. P. Nature 1964, 201, 68.
13. Kinssinger, H. E. Anal Chem 1957, 29, 1702.
14. Fraga, F.; Rodríguez-Núñez, E. J Appl Polym Sci 2001, 80, 776.
15. Doyle, C. D. J Appl Polym Sci 1961, 5, 285.
16. Phadnis, A. B.; Deshpande, V. V. Thermochim Acta 1983, 62, 361.
17. Zhao, X. J.; Liu, B. Y.; Wang, X. H.; Zhao, D. Q.; Wang, F. S. Chinese Patent Application Open Number, 1998, CN1257885A.
18. Zhao, X. J.; Liu, B. Y.; Wang, X. H.; Zhao, D. Q.; Wang, F. S. Chinese Patent Application Open Number, 1998, CN1257753.
19. Li, S. D.; Yu, P. H.; Cheung, M. K. J Appl Polym Sci 2001, 80, 2237.
20. Núñez, L.; Fraga, F.; Núñez, M. R.; Castro, A.; Fraga, L. J Appl Polym Sci 1999, 74, 2997.
21. Montserrat, S.; Málek, J.; Colomer, P. Thermochim Acta 1998, 313, 83.
22. Thermal Analysis—Techniques & Applications; Charsky, E. L.; Warrington, S. B, Eds.; Royal Society of Chemistry: London, 1992; p 52.
23. Straszko, J.; Olszak-Humienik, M.; Mozejko, J. Thermochim Acta 1997, 292, 145.